Exquisitely accurate energies for the general quartic oscillator

Pavel Okun, Kieron Burke
Department of Chemistry, University of California, Irvine, CA 92697, USA and
Departments of Physics and Astronomy and of Chemistry
(Dated: Monday 31st August, 2020)

Recent advances in the asymptotic analysis of energy levels of potentials produce relative errors in eigenvalue sums of order 10^{-34}, but few non-trivial potentials have been solved numerically to such accuracy. We solve the general quartic potential (arbitrary linear combination of x^2 and x^4) beyond this level of accuracy using a basis of several hundred oscillator states. We list the lowest 20 eigenvalues for 9 such potentials. We confirm the known asymptotic expansion for the levels of the pure quartic oscillator, and extract the next 2 terms in the asymptotic expansion. We give analytic formulas for expansion in up to 3 even basis states. We confirm the virial theorem for the various energy components to similar accuracy. The sextic oscillator levels are also given. These benchmark results should be useful for extreme tests of approximations in several areas of chemical physics and beyond.

1. INTRODUCTION

Since the early days of quantum mechanics, potentials with analytic solutions have played a crucial role in providing both insight into more complex problems, and benchmarks for more general quantum solution methods [1, 2]. The quartic oscillator is iconic in being a simple potential without a built-in length scale which does not have a simple analytic solution [3–7]. The general quartic oscillator (adding both quadratic and linear terms) is not scale-invariant, and has been studied in many different contexts in physics [8–10]. In particular, the Mexican hat shape of symmetric double wells is a paradigm of simple symmetry breaking [8, 11].

In chemical physics, the double well provides important tests of theories of tunneling in quantum nuclear dynamics of liquids [8, 11, 12]. In particle physics, it is a prototype of symmetry breaking, such as occurs in simple field theories [13, 14]. In mathematical physics, it is a simple case to test and explore asymptotic approximations [15]. Asymptotic analysis, especially hyperasymptotics, can yield exquisitely accurate approximations [16–19]. In the past, many developments and tests of these methods have been applied to scale invariant potentials [20–22], but the general quartic oscillator provides opportunities to look at more complex cases.

Recent work on one-dimensional potentials [20–22] has established a deep explicit connection between the gradient expansion of density functional theory and asymptotic expansions in powers of $\hbar$ [23]. In one case fractional errors were below the picoyocto range, i.e., of order 10^{-33} [22]. To further develop and test methods in this area, there is a need for benchmark calculations of this level of accuracy for non-trivial potentials. This exceeds even quadruple precision on standard computers, rendering standard numerical algorithms, even pushed to their convergence limits, difficult to apply. There is also a new area of application: The breaking of symmetry is a simple prototype of a bond breaking, in which electrons localize in two separate wells [24]. Such bond breaking is very difficult to model with standard semilocal density functionals, and their failure has been traced back to the change in asymptotic expansions in going from one well to two[21]. In some simple situations, benchmark electronic structure calculations have been performed to this level of accuracy (or higher) for systems with a few electrons [25]. But the purpose of the present study (and many previous ones) is to explore the underlying principles behind asymptotic (and other) approximation schemes, so as to improve the accuracy of less expensive quantum solvers, such as density functional theory, which can then be applied to much larger systems. The benchmark data here provides a quick reference for those exploring basic questions with analytic one-dimensional models.

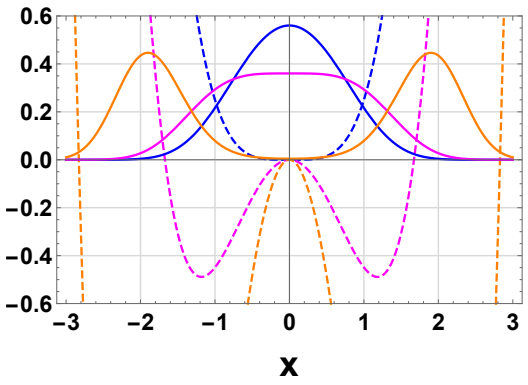

FIG. 1. Ground state densities (solid) and potentials (dashed). Legend: $\lambda = 0$ (blue), $\lambda = \lambda_c$ (magenta), $\lambda = 4$ (orange).

In order to generate such benchmarks and as a simple example, we consider the generalized quartic oscillator potential:

$$v_\lambda(x) = \frac{x^4}{4} - \lambda\frac{x^2}{2}, \tag{1}$$

where λ is a real number, either positive or negative. For $\lambda = 0$, this is a pure quartic oscillator, which has been the subject of many investigations. In this paper we will present the pure quartic oscillator energies for more states and to more digits than previously computed in Refs. [3–5]. We also numerically examine the WKB series for the quartic oscillator closely following Bender & Orszag's book [3]. Previous investigations of the WKB approximation of

the quartic oscillator can be found in Refs. [9, 26–29]. We examine the variation of the energy with λ and the effect of a linear term as in Ref. [9]. Our exact energies can be used as inputs to test the semiclassical analysis of Ref. [30]. Other methods of estimating quartic oscillator energies are described in Refs. [3, 4, 29, 31–33]. The exact solution of the quartic oscillator was studied in Refs. [6, 7]. For $\lambda < 0$, the minimum is always at $x = 0$, with vibrational frequency $\sqrt{|\lambda|}$. For $\lambda > 0$, the most interesting case, two distinct wells appear, with minima at $\pm\sqrt{\lambda}$, and frequency $\sqrt{2\lambda}$. Fig. 1 illustrates some results, showing the density of the ground state and the well for three values of λ: 0, λ_c (the critical value of λ at which the ground state energy is zero), and 4. The first is similar in shape to a harmonic oscillator, but with steeper walls, and the density decays more rapidly. The second is particularly flat, as the energy is exactly zero. The third is a typical double-well structure, with two well-localized densities on each side, and a small 'overlap' at $x = 0$. Thus there is a transition from one well to two, and simple symmetry breaking. Following the behavior of asymptotic expansions with the variation of λ is a toy problem relevant to many fields [15].

In this paper, we show how to calculate extremely accurate results for these potentials using a symbolic manipulation code, such as Mathematica, where manipulations can be performed with an arbitrary number of digits. We summarize results in the main text, and provide some analysis of various regimes. In the supplementary information, we give many tables of results to many digits of accuracy.

2. METHOD

Our Schrödinger equation is (in units where $\hbar = m = 1$)

$$-\frac{1}{2}\frac{d^2\psi}{dx^2} + v(x)\psi(x) = \epsilon\psi(x), \tag{2}$$

so all energies are in Hartrees, all distances in Bohr radii. We expand the eigenfunctions in a basis of harmonic oscillator states, where ω can be freely chosen. The Hamiltonian is pentadiagonal, with only a few non-zero matrix elements no more than 2 double-steps off the diagonal. The nonzero matrix elements of the Hamiltonian in the harmonic basis are $H_{n,n+2k} = h_k\sqrt{n_k}/16\omega^2$ where $h_2 = 1$ and

$$\begin{aligned} h_0 =& 4\omega(\omega^2 - \lambda)(2n+1) + 3(2n^2+2n+1), \\ h_1 =& 2[2n + 3 - 2\omega(\lambda + \omega^2)], \end{aligned} \tag{3}$$

and we use the shorthand

$$\alpha_p = \prod_{m=1}^{p}(\alpha + m), \qquad \alpha_0 = 1. \tag{4}$$

We closely follow Ref. 5 and use the Eigensystem function in Mathematica to diagonalize this matrix for various values of λ and choices of ω [34]. We denote by N_B the number of basis functions included in the calculation (both odd and even, since we did not take advantage of parity). Our default choice of $[\omega/N_B]$ is [2/200] but we use [2/400] as a baseline for 'exact' energies, and report errors relative to those values.

A special case is $\epsilon = 0$ for the ground state (magenta in Fig. 1). This happens at $\lambda = \lambda_c$ which we found using a golden section search to be $1.39825854552989553025859471872183126043 96$, at which the ground state energy is -3.955×10^{-41}. For a different way of finding energies of oscillators of order x^{2M} using exact quantization conditions see Refs. [32, 33]; for an approach using lower bounds see Ref. [31].

3. RESULTS

In this section, we report many different results that may be of interest to different communities under different circumstances. In each case, we also provide a minimal analysis.

3.1. Energetics for different potentials

Here, we simply survey the behavior of the energies and eigenfunctions for various values of λ. Our focus is primarily on positive values of λ, which produce the Mexican hat double-well potential.

n	$\lambda = -1$	$\lambda = 0$	$\lambda = 2$	$\lambda = 4$
0	0.62092703	0.42080497	-0.29952137	-2.66144807
1	2.02596616	1.50790124	0.04637108	-2.65173172
2	3.69845032	2.95879569	1.22797281	-0.51029304
3	5.55757714	4.62122032	2.45984143	-0.18078943
4	7.56842287	6.45350993	3.93826197	1.16951434
5	9.70914788	8.42845388	5.58129195	2.36439189
6	11.96454362	10.52783077	7.36888889	3.83579483
7	14.32326520	12.73833694	9.28322263	5.44300452
8	16.77645279	15.04975293	11.31134968	7.18323497
9	19.31695430	17.45393416	13.44312537	9.03984811

TABLE I. The energies at various values of λ. See Table S1 for more values of λ, more states, and more digits.

Our first results are the energetics of the first several eigenstates of the generalized quartic oscillator. These values are given to 8 digits in Table I for four values of λ. In Table S1 in the supplementary information, we give 40 digits for 9 values of λ for the first 20 eigenvalues. Here $\lambda = 0$ corresponds to the pure quartic oscillator. As λ grows, the eigenvalues inside the double well come in pairs, with ever smaller splitting.

We also show the first three stationary states and potentials at various values of λ in Fig. 2. As λ grows, the ground-state wavefunction develops a minumum at the origin, and the first excited state almost matches it in the bulk of the minimum. By $\lambda = 8$, the wavefunctions are almost indistinguishable, except for their sign.

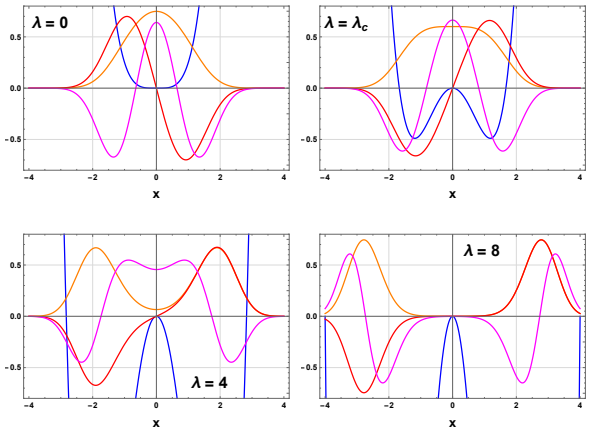

FIG. 2. First three eigenfunctions (orange, red, magenta) with potentials (blue) at various values of λ.

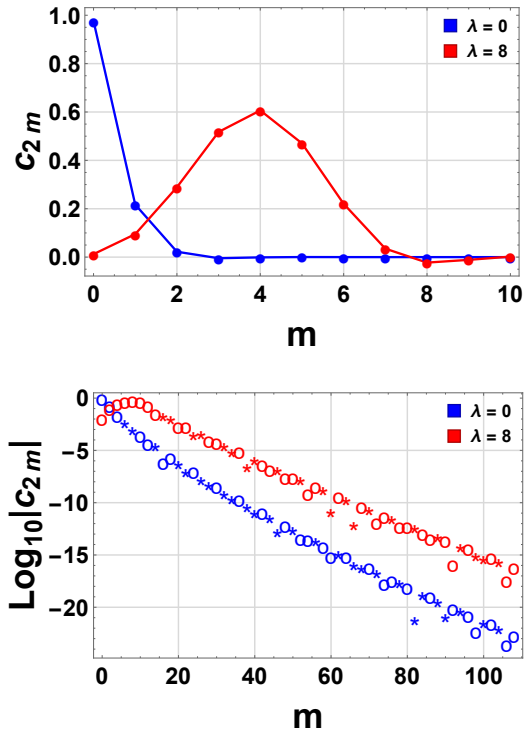

FIG. 3. Behavior of the coefficients of the ground-state wave function for the pure quartic oscillator (blue) and double-well potential (red, $\lambda = 8$) in the basis [2/200]. In the lower panel stars and open circles denote c_{2m} of opposite signs. See Table S2 for more digits.

In Fig. 3 we show the overlap c_m of the ground-state wave function with even oscillator states in a basis of [2/200] for two values of λ. The pure quartic oscillator is dominated by the ground-state of the harmonic oscillator, with overlap close to 1, but the magnitude of the double-well coefficients grows before ultimately decaying. In the lower panel, we show that the overlaps decay exponentially, but with varying signs. The broken symmetry well has overlaps that decay significantly more slowly (about 5 orders of magnitude larger).

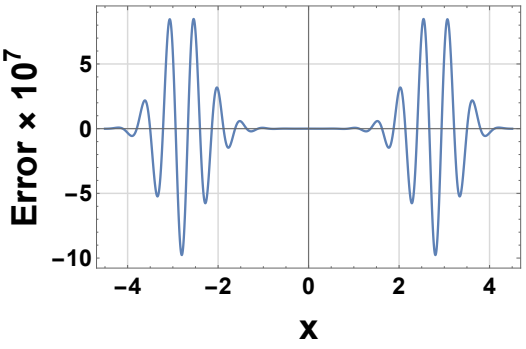

FIG. 4. The error in the ground state density for $\lambda = 8$ calculated with the first 20 coefficients c_{2m} in Table S2.

Lastly, we plot the error in the ground-state density calculated with the first 20 coefficients of [2/200] in Fig. 4 for the double well potential ($\lambda = 8$). This is not the error of the basis set, but simply the error caused by truncation after 20 levels. The error is very small, oscillates in space, and is localized in the two different wells.

3.2. Satisfaction of virial theorem

The virial theorem [35] is a useful check on the accuracy of eigenstates in a basis. It is particularly simple here, as the potential is a sum of two powers of x. For $v_\lambda(x)$, the virial theorem requires, for any eigensolution

$$\langle p^2 \rangle + \lambda \langle x^2 \rangle = \langle x^4 \rangle , \tag{5}$$

with nonzero matrix elements

$$\begin{aligned} \bar{x}_0^2 =& \bar{p}_0^2 = 2n+1,\ \bar{x}_1^2 = -\bar{p}_1^2 = \sqrt{n_2}, \\ \bar{x}_0^4 =& 3(2n^2+2n+1),\ \bar{x}_1^4 = 2\sqrt{n_2}(2n+3),\ \bar{x}_2^4 = \sqrt{n_4}, \end{aligned} \tag{6}$$

where $\bar{x}_k = x_{n,n+2k}\sqrt{2\omega}$ and $\bar{p}_k = p_{n,n+2k}\sqrt{2/\omega}$. In particular, at λ_c, we find the simple formula:

$$\frac{\langle p^2 \rangle}{\langle x^2 \rangle} = \frac{\lambda_c}{3}. \tag{7}$$

In Table II we show how closely our solutions satisfy Eq. 5. This confirms that with [2/200] we have a very good approximation to the exact ground states. Eq. 7 is satisfied to 39 decimal places.

3.3. Tunneling between wells

In this section, we examine both the zero point energy and the tunneling between the symmetric wells that occur for positive λ. As mentioned before, the vibrational frequency is $\sqrt{|\lambda|}$ for negative λ, and $\sqrt{2\lambda}$ for positive λ. Fig.

λ	$\langle p^2\rangle$	$\langle x^2\rangle$	$\langle x^4\rangle$	$\langle p^2\rangle+\lambda\langle x^2\rangle-\langle x^4\rangle$
-1	0.7096226227	0.3548402512	0.3547823715	-1.0×10^{-69}
0	0.5610732993	0.4561199557	0.5610732993	-3.8×10^{-68}
$\frac{1}{2}$	0.4859528308	0.5399767422	0.7559412019	-3.2×10^{-66}
1	0.4187530838	0.6673186910	1.0860717748	9.6×10^{-67}
λ_c	0.3828873103	0.8214946618	1.5315492412	0.0×10^{-40}
2	0.4053838252	1.2071184727	2.8196207705	1.2×10^{-63}
4	1.2230281089	3.5787191485	15.5379047030	9.7×10^{-60}
8	1.9338080508	7.7414002199	63.8650098103	-1.6×10^{-51}

TABLE II. Expectation values and their virial sum for different wells with [2/200]. See Table S3 for more digits.

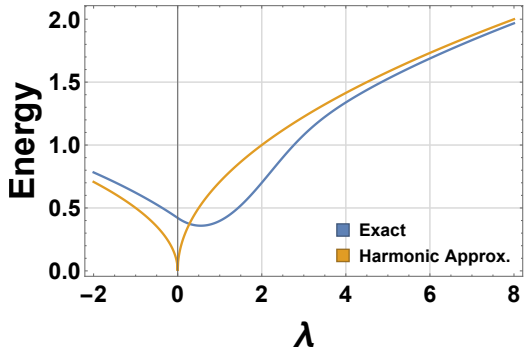

FIG. 5. Exact zero point energy and it's harmonic approximation. See Table S4 for many digits.

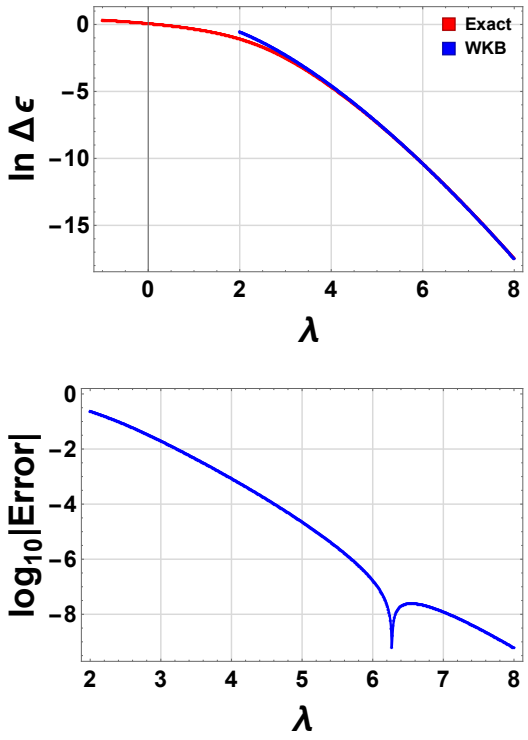

FIG. 6. The upper panel compares the exact $\Delta\epsilon$ splitting with its WKB approximation in Eq. 11. The lower panel shows the error of the WKB approximation. See Table S4 for the exact $\Delta\epsilon$ values.

5 shows the exact zero-point energy and it's harmonic approximation, which becomes accurate as $|\lambda|$ grows.

Less trivial is the tunneling between the broken-symmetry wells. A simple WKB analysis[35] yields

$$\epsilon_\pm = \frac{\omega_0}{2} \mp \frac{\omega_0}{2\pi} e^{-\phi}, \tag{8}$$

for the lowest two levels, where ω_0 is the vibrational frequency, and ϕ is the decay rate for tunneling, evaluated on the ground-state energy. The splitting is

$$\Delta\epsilon = \frac{\omega_0}{\pi} e^{-\phi(\lambda)}, \tag{9}$$

and $\omega_0 = \sqrt{2\lambda}$ in the harmonic approximation. Here ϕ is the integral of the absolute value of the momentum $p(x) = \sqrt{2[\epsilon - v_\lambda(x)]}$ over the classically forbidden region between the two wells

$$\phi = 2\int_0^{x_1} dx \sqrt{2[v_\lambda(x) + \lambda^2/4 - \omega_0/2]}, \tag{10}$$

where $x_1 = \sqrt{\lambda - 2^{3/4}\lambda^{1/4}}$ is the inner turning point and $-\lambda^2/4+\omega_0/2$ is the harmonic approximation to the ground state energy. For the approximation to be meaningful, the inner turning point must be positive, so that $\lambda > 2$. The appendix shows how to find the asymptotic behavior of the splitting for large λ:

$$\Delta\epsilon = \frac{2^{11/4}\sqrt{e}}{\pi}\lambda^{5/4}\exp\left(-\frac{(2\lambda)^{3/2}}{3}\right). \tag{11}$$

Fig. 6 shows just how accurate this approximation is. We have confirmed this expansion numerically.

3.4. Sextic oscillator

In this section, we apply exactly the same technology to finding the energies of the sextic oscillator:

$$v(x) = \frac{x^6}{6}. \tag{12}$$

The quartic and sextic oscillators both belong to the class of potentials whose exact solutions are given by Heun's special function [36]. In our harmonic basis, the nonzero Hamiltonian matrix elements are $H_{n,n+2k} = \sqrt{n_{2k}}h_k^{(6)}/48\omega^3$ where $h_3^{(6)} = 1$ and

$$\begin{aligned} h_0^{(6)} &= (2n+1)[10n(n+1) + 3\left(4\omega^4+5\right)], \\ h_1^{(6)} &= 3[5n(n+3) - 4\omega^4 + 15], \\ h_2^{(6)} &= 3(2n+5), \end{aligned} \tag{13}$$

i.e., they go one more step away from the diagonal. The energies of the first twenty sextic oscillator states are given in Table III.

n	Energy
0	0.43493087870825459239874279292555363392774
1	1.64831106336517093605783724089979389227058
2	3.44702671416130810318518311192928729955987
3	5.67413742993262212079377794412021425830389
4	8.24959885963474520141239532995124004167 30
5	11.13145828009733275940992958109248369395669
6	14.28988270823523783646886992792593890944806
7	17.70235221954562079900780369145795203975459
8	21.35111714819949016424850927302262003053565
9	25.22171285703672981248414385975444098122878
10	29.30205319182515264341685743177538338413530
11	33.58184072441714447659452964789566752711547
12	38.05216382472115780004920306874727674910548
13	42.70521061321923679887306117322169371214762
14	47.53405945114494426110319556943507798525146
15	52.53252145969695924991153932257382502470230
16	57.69501952928699913809886057200837269497456
17	63.01649360693670075261996021857703983520713
18	68.49232534279718129547616418400704809075654
19	74.11827728288342368118468014333735452468298

TABLE III. First twenty energies of the sextic oscillator calculated with [2/800]. The energies are accurate to all 41 digits shown.

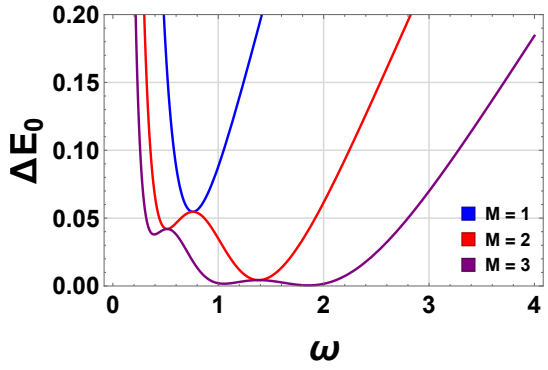

FIG. 7. The errors of the analytic expressions for the approximate ground state with 1, 2, and 3 even basis functions and $\lambda = \lambda_c$.

3.5. Analytic results for a few states

It can often be useful to find an approximate solution using just a few basis functions, instead of hundreds. Here we give analytic formulas for the lowest lying even energies as functions of ω and λ when only 1, 2, and 3 even oscillator states are used. These expressions can be useful for quick estimates of low-lying eigenvalues. The approximate ground-state energy with one even basis function is

$$\epsilon_0 = \frac{3}{16\omega^2} + \frac{\omega}{4} - \frac{\lambda}{4\omega}, \qquad (N_B = 1). \tag{14}$$

The approximate ground- and second-excited states with two even basis functions are:

$$\begin{aligned} \epsilon_\pm &= \frac{3\left(\omega^2 - \lambda\right)}{4\omega} + \frac{21 \pm 2\sqrt{D}}{16\omega^2}, \qquad (N_B = 3), \\ D &= 8\omega[3\omega\left(\lambda^2 + \omega^4 + 2\omega\right) - 2\lambda\left(\omega^3 + 6\right)] + 99. \end{aligned} \tag{15}$$

With three even basis functions the first three approximate even state energies are $(n = 0, 2, 4)$:

$$\begin{aligned} \epsilon_n &= \frac{1}{48\omega^2}\Bigg[15(11 - 4\lambda\omega + 4\omega^3) \\ &\quad - (-1)^{\delta_{n,2}} 8\sqrt{6D}\cos\left(\frac{\phi}{3} + \frac{(n+1)\pi}{6}\right)\Bigg], \ (N_B = 5), \\ D &= 15[\omega^2\left(\lambda^2 + \omega^4 + \omega\right) - 7\lambda\omega + 13] - 2\lambda\omega^4, \\ \sin\phi &= \frac{9B}{8\sqrt{6D}D}, \\ B &= 20\lambda\omega\left(\lambda\omega[51 - 4\omega(\lambda + \omega^2)] + 2[2\omega^6 + 7(\omega^3 - 15)]\right) \\ &\quad + 4\omega^6\left(20\omega^3 - 57\right) + 5575. \end{aligned} \tag{16}$$

At λ_c (Fig. 7), the least error in the ground state energy is 5.467×10^{-2} at $\omega = 0.7595$ with Eq. 14, 4.320×10^{-3} at $\omega = 1.383$ with Eq. 15, and 4.563×10^{-4} at $\omega = 1.854$ with Eq. 16.

3.6. Error dependence on ω

In this paper we have usually set the basis set angular frequency ω to 2. Now we analyze what happens to the error of the ground and a highly excited state of the pure quartic oscillator as ω is varied. The error as a function of ω for a fixed number of basis states is complicated and has several local minima, as we found in the previous section. Nevertheless there is a clear trend for the pure quartic oscillator as seen in Fig. 8: the error tends to level off to a very low value as ω increases, though it must increase if ω becomes too large. The error for the 19th excited state is orders of magnitude greater than that of the ground state with e.g., $N_B = 40$. For our purposes, the value of $\omega = 2$ yielded sufficient accuracy for the basis sets we could afford.

3.7. Quartic potential as perturbation

Consider the case where λ is large and negative, and treat the quartic potential as a perturbation. This problem and it's analytic structure was studied in Refs. [27, 28, 37]. The zeroth, first, and second order contributions to the energies

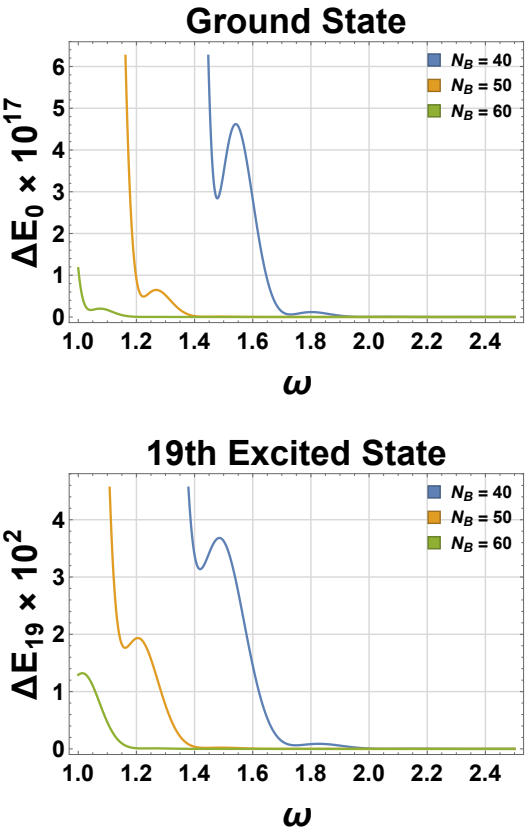

FIG. 8. The errors of the ground state and 19th excited state (i.e. 10th odd state) as a function of ω. See Table S5 for more digits.

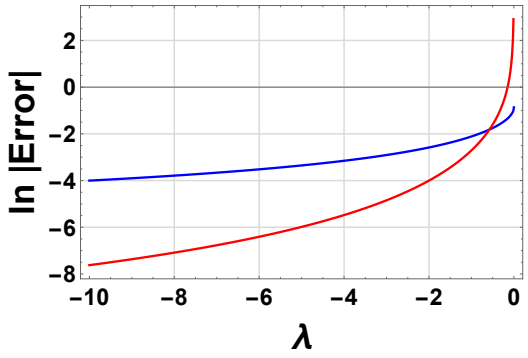

FIG. 9. The error in the ground state energy from zeroth (blue) and first order (red) perturbation theory. See Table S6 for accurate numbers.

are

$$\epsilon_n^{(0)} = \left(n+\frac{1}{2}\right)\sqrt{|\lambda|},$$
$$\epsilon_n^{(1)} = \frac{3(2n^2+2n+1)}{16|\lambda|}, \qquad (17)$$
$$\epsilon_n^{(2)} = -\frac{(1+2n)[17n(n+1)+21]}{128|\lambda|^{5/2}}.$$

n	Energy	difference
0	−2.84178633947585932025083089644391799927051	−0.1803382726
1	−2.47315425631802332765380889849256442811375	0.1785774606
2	−0.55873199537080776530382207755703245716816	−0.0484389572
3	−0.13874405574419168918357404272418272068978	0.0420453773
4	1.16447030692387601517830930663899021569773	−0.0050440297
5	2.36573532391604302707250344355822369758964	0.0013434316
6	3.83568104437914171468097998090919165511556	−0.0001137882
7	5.44302728549612071643675096706241920608503	0.0000227623
8	7.18320046060050124539642226054074137331752	−0.0000345135
9	9.03979350957144560421088106446755353161811	−0.0000546026
10	11.00244857292039554353678211539683848606553	−0.0000702608
11	13.06271608472508976557198671004627390279753	−0.0000808253
12	15.21369451941728871017509326975221513855338	−0.0000881381
13	17.44958477274837116578655941806092145442188	−0.0000931621
14	19.76542796609356112334994801927133021018867	−0.0000965616
15	22.15692272774436386892142052150687339550426	−0.0000987886
16	24.62029451810540168163027589352125330801114	−0.0001001588
17	27.15219883683433104396784761809263032892086	−0.0001008965
18	29.74964765111306868111782309284631425560723	−0.0001011638
19	32.40995226660074725753866259978103913402690	−0.0001010795

TABLE IV. The first twenty energies when $\lambda = 4$ and $\alpha = 0.1$ calculated with [3/200]. The difference from $\alpha = 0$ is reported. All energies are accurate to the 41 digits given.

Fig. 9 shows the resulting error in the ground state energy.

3.8. Asymmetric wells

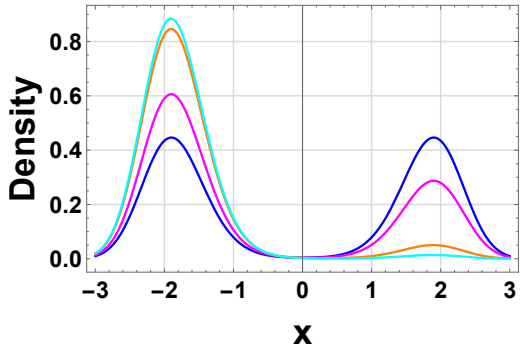

FIG. 10. The ground state density with $\lambda = 4$ and various values of α: 0 (blue), 0.001 (magenta), 0.005 (orange), 0.01 (cyan).

We now examine the effect of breaking the symmetry of $v_\lambda(x)$ by adding a linear term

$$v_{\lambda,\alpha}(x) = \frac{x^4}{4} - \lambda\frac{x^2}{2} + \alpha x. \qquad (18)$$

We only examine the case $\lambda = 4$. In Table IV, we show both the energies for the case $\alpha = 0.1$ and their difference from the unperturbed case $\alpha = 0$. As one side of the well is depressed and the other elevated, for the low-lying states, the differences alternate in sign. As one goes further up the well, eventually all states are lower than their symmetric counterparts.

In Fig. 10 we show how the ground state density varies as α is increased. Even a very small value of α causes sub-

stantial asymmetry in the ground-state density, with almost all the weight in the lower well when $\alpha = 0.1$.

3.9. Asymptotic analysis of pure quartic oscillator

n	k_n	l_n
0	1	3
1	-1	4
2	11	3×2^9
3	$7 \times 11 \times 61$	$3 \times 5 \times 2^{11}$
4	$-5 \times 13 \times 17 \times 353$	7×2^{19}
5	$-11^2 \times 19 \times 23 \times 1009$	3×2^{21}
6	$5 \times 17 \times 29 \times 49707277$	$3 \times 11 \times 2^{28}$
7	$3^4 \times 7 \times 19 \times 23 \times 31^2 \times 109 \times 1429$	13×2^{30}
8	$-7 \times 11 \times 29 \times 37 \times 41 \times 4477909193$	3×2^{39}
9	$-5 \times 11 \times 19 \times 23 \times 31 \times 43 \times 47 \times 1489 \times 6397 \times 8263$	17×2^{41}
10	$7 \times 29 \times 37 \times 41 \times 53 \times 59 \times 3618497 \times 83558311$	$3 \times 19 \times 2^{48}$

TABLE V. The known A_{2n} are given by the k_n and l_n in $A_{2n} = (k_n/l_n)\sqrt{\pi}R^{(-1)^n}$ where $R = \Gamma(1/4)/\Gamma(3/4)$.

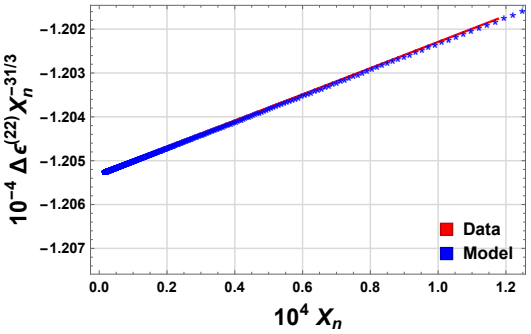

FIG. 11. The coefficients B_{22} and B_{24} are obtained by a linear fit to the above data. We plot $B_{22} + B_{24}X_n$ to show how closely this model matches the data.

The asymptotic solution of the pure and generalized quartic oscillator has been studied many times before [3, 9, 10, 26]. We analyze only the pure quartic oscillator and closely follow Bender & Orszag [3]. The WKB series for a pure quartic oscillator with potential $v(x) = x^4/4$ yields

n	A_{2n}	B_{2n}
0	1.74803836952807987364	1.09253465015618881971
1	−0.14976752934194902593	0.03864050890478489138
2	0.03755551184532984104	−0.00385400310372957406
3	0.09159610485926231443	−0.00192912270049430287
4	−0.55736698690956972061	0.00455965708128336316
5	−5.08024277232829207859	0.01110530044025892883
6	72.53628245858812264379	−0.05611473947869961072
7	1591.77267377039864942443	−0.34434940280222393316
8	−48231.49420089254973409982	3.51923362542214395736
9	−1899239.99920378994311897265	39.91240769625859000539
10	95166684.23238064054845710849	−660.60215595012034723938

TABLE VI. The known WKB coefficients for the pure quartic oscillator reported to twenty digits.

the implicit formula

$$\sum_{m=0}^{\infty} A_{2m}(4\epsilon^{3/2})^{1/2-m} = \left(n+\frac{1}{2}\right)\pi, \tag{19}$$

with the known A_{2n} reported in Table V and in Refs. [3, 38]. One can invert this implicit expression to an explicit formula for each level:

$$\epsilon_n = 2^{-1/3}\sum_{m=0}^{\infty} B_{2m}\left(n+\frac{1}{2}\right)^{4/3-2m}. \tag{20}$$

We give the known A_{2n} and B_{2n} coefficients numerically in Table VI to twenty decimal places. The analytic forms of the B_{2n} coefficients are given by

$$B_{2n} = (-1)^{\lfloor n/2\rfloor}\frac{\pi^{2-n}\beta_n}{18^{1/3}\Gamma(1/4)^{8/3}}, \tag{21}$$

where the β_n are polynomials of order $\lfloor n/2\rfloor$ in γ:

$$\beta_n = C_n\sum_{k=0}^{\lfloor n/2\rfloor} a_{n,k}\gamma^k, \tag{22}$$

where $\gamma = \Gamma(1/4)^8/\pi^4$. This allows the 11 known β_{2n} to be given by the constants in Table VII.

We can use our highly accurate energies to extract higher order coefficients. We define the deviation from the $2m$-th order WKB approximation as

$$\Delta\epsilon_n^{(2m)} = \epsilon_n - \epsilon_{WKB,n}^{(2m-2)}, \tag{23}$$

which, according to Eq. 20, has the asymptotic form

$$\Delta\epsilon_n^{(2m)} = B_{2m}X_n^{m-2/3} + B_{2m+2}X_n^{m-2/3+1} + ..., \tag{24}$$

where

$$X_n = \left(n+\frac{1}{2}\right)^{-2}, \tag{25}$$

yielding

$$\Delta\epsilon_n^{(2m)}X_n^{2/3-m} = B_{2m} + B_{2m+2}X_n + B_{2m+4}X_n^2 + ... \tag{26}$$

Thus by calculating accurate energies, multiplying them by $X_n^{2/3-m}$, and fitting to a line, we confirm the WKB coefficients up to twentieth order and find the next two coefficients numerically, as shown in Fig. 11. Our most accurate approximations to B_{22} and B_{24} were calculated using [3/3000] to be $B_{22} = -1.2052792 \times 10^4$ and $B_{24} = 2.98 \times 10^5$, which are accurate to the number of digits shown. To speed up the calculation we took advantage of parity and calculated the odd and even energies separately using the ParallelTable function in Mathematica [34].

n	C_n	$a_{n,0}$	$a_{n,1}$	$a_{n,2}$	$a_{n,3}$	$a_{n,4}$	$a_{n,5}$
0	9	1					
1	1	1					
2	1/72	5	11/192				
3	11/972	−1	93/640				
4	17/559872	−77	539/20	102829/86016			
5	23/5038848	119	−3289/48	28171999/430080			
6	29/1088391168	5083	−661089/160	6734014687/716800	49829732957/90832896		
7	1/1224440064	−43355	2931929/64	−10264192781/61440	492349052125069/1349517312		
8	41/176319369216	−164749/4	806113/15	−262775969173/983040	787570022698313/527155200	45866361756966241/355140108288	
9	47/211583430592	3230513/27	−7446461/40	4267944409223/3686400	−1335041940357576377/120766464000	490756642086934461093/98107454914560	
10	53/1371059415023616	58397735/3	−9015402055/256	89325797863511/344064	−955865010579864937/268369920	14075604276965734971467 89/32702484971520	562019233992163451044 1141/1187588522115072

TABLE VII. The constants yielding the β_n via Eq. 22.

4. CONCLUSIONS

We have used Blinder's method to extract many quantities from the general quartic oscillator to many digits [5]. We have considered many distinct limits and scenarios where these benchmark results might be useful. We have covered energetics of eigenstates, the virial theorem, tunneling between wells, the sextic oscillator, analytic forms in a few basis functions, error dependence on choice of ω, perturbation theory in the quadratic term, asymmetric wells, and asymptotic analysis of WKB results for the pure quartic case. In all cases, we have provided preliminary analysis and compared with the exact results. We expect future studies in specific areas to perform more thorough analysis in the cases considered here, and in others we have not anticipated.

5. FUNDING INFORMATION

This research was supported by NSF (CHE 1856165).

[1] E. Schrödinger, Phys. Rev. **28**, 1049 (1926), URL https://link.aps.org/doi/10.1103/PhysRev.28.1049. 1

[2] N. Rosen and P. M. Morse, Phys. Rev. **42**, 210 (1932), URL https://link.aps.org/doi/10.1103/PhysRev.42.210. 1

[3] C. M. Bender and S. A. Orszag, *Advanced mathematical methods for scientists and engineers* (Springer, 1999). 1, 2, 7

[4] C. E. Reid, Journal of Molecular Spectroscopy **36**, 183 (1970), ISSN 0022-2852, URL http://www.sciencedirect.com/science/article/pii/0022285270901037. 2

[5] S. M. Blinder, *Eigenvalues for a pure quartic oscillator* (2019), 1903.07471. 1, 2, 8

[6] W. Lay, Journal of Mathematical Physics **38**, 639 (1997), URL https://doi.org/10.1063/1.531857. 2

[7] K. Bay and W. Lay, Journal of Mathematical Physics **38**, 2127 (1997), URL https://doi.org/10.1063/1.531962. 1, 2

[8] J. Joger, A. Negretti, and R. Gerritsma, Physical Review A **89** (2014), ISSN 1094-1622, URL http://dx.doi.org/10.1103/PhysRevA.89.063621. 1

[9] E. Delabaere and F. Pham, Annals of Physics **261**, 180 (1997), ISSN 0003-4916, URL http://www.sciencedirect.com/science/article/pii/S0003491697957377. 2, 7

[10] C. M. Bender and T. T. Wu, Phys. Rev. D **7**, 1620 (1973), URL https://link.aps.org/doi/10.1103/PhysRevD.7.1620. 1, 7

[11] S. K. S. D. L. Meier, Thomas; Petitgirard, Nature Communications **9** (2018), URL https://doi.org/10.1038/s41467-018-05164-x. 1

[12] Y. Fujimura and H. Sakai, *Electronic and Nuclear Dynamics in Molecular Systems* (WORLD SCIENTIFIC, 2011), https://www.worldscientific.com/doi/pdf/10.1142/7119, URL https://www.worldscientific.com/doi/abs/10.1142/7119. 1

[13] R. Dutt, A. Gangopadhyaya, A. Khare, A. Pagnamenta, and U. Sukhatme, Phys. Rev. A **48**, 1845 (1993), URL https://link.aps.org/doi/10.1103/PhysRevA.48.1845. 1

[14] F. Cooper, A. Khare, and U. Sukhatme, Physics Reports **251**, 267 (1995), ISSN 0370-1573, URL http://www.sciencedirect.com/science/article/pii/037015739400080M. 1

[15] I. Aniceto, G. Basar, and R. Schiappa, Physics Reports **809**, 1 (2019), ISSN 0370-1573, a primer on resurgent transseries and their asymptotics, URL https://doi.org/10.1016/j.physrep.2019.02.003. 1, 2

[16] O. Costin, *Asymptotics and borel summability* (Chapman & Hall/CRC Press, Boca Raton, 2009), ISBN 9781420070316. 1

[17] M. V. Berry and C. J. Howls, Physics World **6**, 35 (1993).

[18] M. V. Berry and C. J. Howls, Proceedings of the Royal Society of London. Series A: Mathematical and Physical Sciences **430**, 653 (1990), https://royalsocietypublishing.org/doi/pdf/10.1098/rspa.1990.0111, URL https://royalsocietypublishing.org/doi/abs/10.1098/rspa.1990.0111.

[19] M. V. Berry and K. E. Mount, Reports on Progress in Physics **35**, 315 (1972), URL https://doi.org/10.1088%2F0034-4885%2F35%2F1%2F306. 1

[20] K. Burke, arXiv:2005.08403 (2020). 1

[21] K. Burke, The Journal of Chemical Physics **152**, 081102 (2020), URL https://doi.org/10.1063/5.0002287. 1

[22] M. V. Berry and K. Burke, Journal of Physics A: Mathematical and Theoretical **53**, 095203 (2020), URL https://doi.org/10.1088%2F1751-8121%2Fab69a6. 1

[23] A. Cangi, D. Lee, P. Elliott, and K. Burke, Phys. Rev. B **81**, 235128 (2010), URL https://link.aps.org/doi/10.1103/PhysRevB.81.235128. 1

[24] A. Cohen, P. Mori-Sánchez, and W. Yang, Phys. Rev. B **77**, 115123 (2008), URL http://link.aps.org/doi/10.

1103/PhysRevB.77.115123. 1
[25] H. Nakashima and H. Nakatsuji, The Journal of Chemical Physics **127**, 224104 (2007), https://doi.org/10.1063/1.2801981, URL https://doi.org/10.1063/1.2801981. 1
[26] A. Voros, Annales de l'I.H.P. Physique théorique **39**, 211 (1983), URL http://www.numdam.org/item/AIHPA_1983__39_3_211_0. 2, 7
[27] C. M. Bender and T. T. Wu, Phys. Rev. **184**, 1231 (1969), URL https://link.aps.org/doi/10.1103/PhysRev.184.1231. 5
[28] C. M. Bender and T. T. Wu, Phys. Rev. Lett. **21**, 406 (1968), URL https://link.aps.org/doi/10.1103/PhysRevLett.21.406. 5
[29] F. T. Hioe and E. W. Montroll, Journal of Mathematical Physics **16**, 1945 (1975), https://doi.org/10.1063/1.522747, URL https://doi.org/10.1063/1.522747. 2
[30] D. Brizuela, Physical Review D **90** (2014), ISSN 1550-2368, URL http://dx.doi.org/10.1103/PhysRevD.90.125018. 2
[31] E. Pollak and R. Martinazzo, The Journal of Chemical Physics **152**, 244110 (2020), https://doi.org/10.1063/5.0009436, URL https://doi.org/10.1063/5.0009436. 2
[32] A. Voros, Journal of Physics A: Mathematical and General **27**, 4653 (1994), URL https://doi.org/10.1088%2F0305-4470%2F27%2F13%2F038. 2
[33] A. Voros, Journal of Physics A: Mathematical and General **32**, 5993 (1999), URL https://doi.org/10.1088%2F0305-4470%2F32%2F32%2F311. 2
[34] W. R. Inc., *Mathematica, Version 11.3*, URL https://www.wolfram.com/mathematica. 2, 7
[35] D. J. Griffiths, *Introduction to quantum mechanics* (Pearson Prentice Hall, 2005). 3, 4
[36] G. Lévai and A. M. Ishkhanyan, Modern Physics Letters A **34**, 1950134 (2019), https://doi.org/10.1142/S0217732319501347, URL https://doi.org/10.1142/S0217732319501347. 4
[37] B. Simon and A. Dicke, Annals of Physics **58**, 76 (1970), ISSN 0003-4916, URL http://www.sciencedirect.com/science/article/pii/000349167090240X. 5
[38] A. Voros, Nuclear Physics B **165**, 209 (1980), ISSN 0550-3213, URL http://www.sciencedirect.com/science/article/pii/0550321380900851. 7
[39] DLMF, *NIST Digital Library of Mathematical Functions*, http://dlmf.nist.gov/, Release 1.0.26 of 2020-03-15, 19.2, URL https://dlmf.nist.gov/19.2. 9
[40] DLMF, *NIST Digital Library of Mathematical Functions*, http://dlmf.nist.gov/, Release 1.0.26 of 2020-03-15, 19.12, URL https://dlmf.nist.gov/19.12. 9

Appendix A: Derivation of asymptotic splitting formula

We now explain how to derive Eq. 11, the asymptotic approximation to $\Delta\epsilon = \epsilon_1 - \epsilon_0$ in the limit $\lambda \to \infty$.

We introduce the shorthand $\eta = (2/\lambda)^{3/4}$ so $\lambda \to \infty \implies \eta \to 0_+$. In terms of η Eq. 10 of the main text becomes

$$\phi(\eta) = \frac{4}{\eta^2}\int_0^{\sqrt{1-\eta}} dx\sqrt{(1-x^2)^2-\eta^2}. \tag{A1}$$

In the limit $\eta \to 0_+$,

$$\phi^{(0)}(\eta) = \frac{4}{\eta^2}\int_0^1 dx(1-x^2) = \frac{(2\lambda)^{3/2}}{3}. \tag{A2}$$

We evaluate Eq. A1:

$$\phi(\eta) = \frac{8}{3\eta^2}\sqrt{1+\eta}F(\eta), \tag{A3}$$

where $F(\eta) = \mathcal{E}(y) - \eta\mathcal{K}(y)$, $y = (1-\eta)/(1+\eta)$ and

$$\mathcal{K}(x) = \int_0^{\pi/2}\frac{d\theta}{f(x,\theta)},\ \mathcal{E}(x) = \int_0^{\pi/2} d\theta f(x,\theta), \tag{A4}$$

with $f(x,\theta) = \sqrt{1-x\sin^2\theta}$ [39]. The following expansion will prove useful shortly:

$$F(\eta) = 1 - \frac{\eta}{2} + \frac{3}{16}\eta^2(1 - 6\ln 2 + 2\ln\eta) + \mathcal{O}(\eta^3), \tag{A5}$$

as $\eta \to 0_+$ [40]. Inserting Eq. A5 into Eq. A3 and expanding around $\eta = 0$, yields

$$\phi^{(2)}(\lambda) = \frac{(2\lambda)^{3/2}}{3} - \frac{3}{4}\ln\lambda - \frac{1}{4}(2 + 9\ln 2). \tag{A6}$$

The above equation combined with Eq. 9 leads to the final result, Eq. 11 of the main text.